

# Superplasticity of ultrafine grained low-alloy steels

## *Superplasticidad de aceros de baja aleación con grano ultrafino*

Sara Fernández<sup>1</sup>, María José Quintana<sup>2</sup>, José Ovidio García<sup>1</sup>, Luis Felipe Verdeja<sup>1</sup>, Roberto González<sup>2</sup>, José Ignacio Verdeja<sup>1</sup>

Recibido: Agosto 2012

Aprobado: Setiembre 2012

**Resumen.-** Los aceros con estructura de grano ultrafino pueden presentar comportamiento superplástico a temperaturas y velocidades de deformación específicas, que faciliten la activación de los mecanismos de deslizamiento de fronteras de grano. El comportamiento superplástico implica deformaciones elevadas por procesos de deslizamiento de fronteras de grano con acomodo de materia por difusión, tal como lo describe el modelo de Ashby-Verrall. El trabajo presenta pruebas de tensión a temperatura elevada en aceros de bajo carbono y baja aleación obtenidos por procesos avanzados de rolado controlados termomecánicamente, mostrando a 800°C elongaciones de hasta el 200%. La microestructura del acero se analizó para poder identificar las fronteras de grano de la ferrita y de la perlita, y su interacción después de que la probeta fue deformada. Las técnicas de microanálisis (óptico y SEM) muestran evidencia de: crecimiento de defectos que impiden alcanzar elongaciones a ruptura mayores, flujo no uniforme (movimiento-rotación relativo de granos próximos entre sí) y deformación intergranular no-superplástica (flujo cuasi-uniforme), resultando todo esto en fractura prematura.

**Palabras clave:** superplasticidad, grano ultrafino, coeficiente  $m$  de velocidad de deformación, deslizamiento de fronteras, aceros de alta resistencia y baja aleación.

**Summary.-** Write Steels with ultrafine grained structure may present superplastic behavior at specific temperatures and strain rates that allow the grain boundary sliding mechanisms to be activated. The superplastic behavior implies deformation to large strains by grain-boundary sliding with diffusional accommodation, as described by the Ashby-Verrall model. The work presents high temperature tension tests in a low carbon, low alloy steel obtained by advanced thermomechanical controlled rolling processes, showing at 800°C elongations as high as 200%. The microstructure of the steel was analyzed in order to identify ferrite and pearlite grain boundaries, and their interaction after the specimens were deformed. Microanalytical techniques (Optical and SEM) show evidence of: damage growth that prevents the development of higher elongations to failure, non-uniform flow (relative movement-rotation of grains in close proximity to each other) and intergranular non-superplastic deformation (quasi-uniform flow); thus leading to premature failure.

**Keywords:** superplasticity, ultrafine grained, strain rate  $m$  coefficient, boundary sliding, high-strength low alloy steels (HSLA steels)

**1. Introduction.-** Superplasticity is the ability of polycrystalline solids (metals) to achieve extremely high and uniform elongations (from 100 to 1000%) when applying tensile stresses. The high dependency between the creep tension stress and the strain rate results in the lack of necking (or a series of diffuse necks) along the test zone of a specimen [1]. From a

<sup>1</sup> E.T.S.I.M.O., Universidad de Oviedo, Independencia 13, Oviedo 33004, Spain, Tel. (34) 985 10-43-03, Fax. (34) 985 10-42-42, lfv@etsimo.uniovi.es

<sup>2</sup> School of Engineering, Universidad Panamericana, Augusto Rodin 498, 03920, México, D.F., Mexico, Tel. (52)55 1251-6859, Fax. (52)55 5482-1600 ext. 6101, robglez@up.edu.mx

microstructural point of view, superplasticity is achieved when two mechanisms take place in the material: grain boundary migration and grain boundary shearing/sliding. Theoretical and microstructural models agree that the most important feature of this behavior is the grain boundary sliding (GBS). Nevertheless, dislocations or diffusion in grains or in zones near grain boundaries are necessary in order to maintain the superplasticity of the material [2].

Four essential characteristics [3] are required in a material for it to be considered superplastic: a stable microstructure of fine equiaxed grains [4],  $m$  coefficient (strain-rate sensitivity exponent;  $\sigma = K \cdot \dot{\epsilon}^m$ ) values between 0.3 and 0.7, slow strain rates ( $10^{-3}$  to  $10^{-5}$  s<sup>-1</sup>) and grain boundaries of the material that allow grain sliding and rotation when stress is applied [5].

In addition to the previous requirements, it is necessary to deform the material at the right temperature which is a fundamental characteristic in some superplastic behavior models, such as the one established by Ashby and Verrall [6]. Their model proposes a theory (Grain Boundary Sliding, Diffusion Accommodated Flow Rate Controlling) to describe superplasticity taking into account two mechanisms: (a) the diffusion-accommodated flow (D-A flow), consisting of GBS along with material transport through grain boundary and bulk crystal diffusion [7] to maintain grain continuity (this phenomena dominates in the low stress regime, strain rates less than  $10^{-5}$  s<sup>-1</sup>) and (b) the ordinary power-law creep (dislocation creep) which is a quasi-uniform flow mechanism that results in grain-elongation as dislocations accumulate as cells, storing energy; this last mechanism dominates at sufficient high stresses (strain rates higher than  $10^{-3}$  s<sup>-1</sup>). In the intermediate stress range, both mechanisms compete in order to achieve the superplastic behavior.

The work presents the high temperature superplastic behavior of an UFG steel microalloyed with Ti-Nb obtained by Advanced Thermomechanical Control Rolling Processes (ATMCRP) at the Arcelor Mittal factory in Veriña (Gijón, Spain), as materials of this type can show this behavior when certain conditions are met. The characteristics of the steel, delivered in the form of 27.6 mm in thickness sheets (around one inch), are described in the experimental procedure. The HSLA steels described in Euronorms 10149-2 and 10051 are examples of these materials, as well as other construction steels or automotive special steels (just as the ones described in the ultralight steel auto body – ULSAB project), resulting in lower cost materials and a step forward in the research for better materials in industry, such as lightweight structures and components with very good weldability and easier to recycle, all of this, reducing the cost of the alloy and meeting high specifications with steels that have a lower amount of alloying elements and that are considered high-tech [8]. Furthermore, ultrafine grained steels (UFG) may be applied in the future in most of the steel markets and can be used in other industrial applications, such as the ones that require superplastic behavior, just as this work demonstrates.

Ultrafine grained steels (grain size  $\bar{d} \approx 1\text{--}5\mu\text{m}$ ) are currently intensively studied worldwide, as they offer a solution to finding very high strength materials. They also present high toughness and are produced from standard steel compositions (which reflects in low cost) [9]. Recent works have shown that the ultrafine grained structure may be obtained in a hot rolling mill by ATMCRP and not only from small scale laboratory tests [4,10]. However, under some circumstances these materials may present an important disadvantage as they exhibit unstable plasticity upon yielding, severely restricting its potential uses [11]. In order to avoid this instability [12] the mechanical behavior of the steel must show a strain hardening coefficient  $n$  (as measured by tension test with the ASTM standard) higher than 0.1, in its hot rolling raw state. If this is achieved, the steel can be used for cold-work operations such as bending, stretching and drawing and in commercial applications such as automotive and other manufacturing industries [4].

A large number of non-ferrous alloys show superplasticity behavior during isothermal tensile testing. This behavior is characterized by large elongations, usually higher than 100% and sometimes reaching 1000% or more. Superplasticity, object of numerous research activities that started in the 1960–1970s, has the following properties:

- high strain rate sensitivity to the flow stress as the essential and unique characteristic of superplasticity [13],
- strong variation of properties as a function of grain size and strain rate [14],
- relevance of grain boundary sliding in the deformation mechanism [3],
- vacuum forming of the metal sheet when deformed against the die [15] and
- grain boundary sliding by diffusion and accommodation processes [6].

In other words, in order for the superplastic behavior to show high strain rate sensitivity, high temperature testing ( $> \frac{1}{2} T_m$ ), a fine microstructure and a relatively low strain rate are required [16-18].

**2. Experimental procedure and Results.**- The specified chemical composition for this steel (in weight %) according to the Euronorm is: C 0.168, Mn 1.361, Si 0.453, P 0.022, S 0.009, Cu 0.026, As 0.003, Al 0.028, Cr 0.035, Ti 0.026, V 0.002, Nb 0.033, Mo 0.004, Ni 0.031, Sn 0.002, Al (soluble) 0.027, B 0.0001, N 0.0055, Zr 0.0000, Ca 0.0001, O 0.0000, H 2.00 ppm, B (soluble) 0.0000. In the same way, the specified mechanical properties are: higher yield stress ( $\sigma_y$ ) = 447 MPa, rupture stress ( $\sigma_{max}$ ) = 567 MPa, yield elongation with  $L_0$  of 50 mm ( $El$ ) = 31 % and impact resistance at -20 °C (KCV) = 96 J.

As an ultrafine grained microstructure is essential to obtain a superplastic behavior, the steel was produced by ATMCRP, which mainly consists of three steps:

1. roughing (in order to reduce the thickness of the slab),
2. waiting period (where the material is cooled between 850 and 1000°C) to obtain Ti and Nb carbides and
3. finishing (where the deformation is accumulated in the austenite in order to obtain the finest ferrite possible after the allotropic transformation), in the same fashion as described in previous works [10].

The samples were obtained from the steel plate in an axis parallel to rolling direction and were machined in a cylindrical shape: 10 mm in diameter and calibrated gage length of either  $L_0 = 57$  or  $L_0 = 30$  mm (ASTM E21-05 standard). High temperature tension tests were made at different temperatures between 600 and 900°C (50°C intervals) and different crosshead speeds in order to define the temperature interval in which the steel would show a superplastic behavior. After defining a temperature in which the material presented this characteristic, more tests were made using different crosshead speeds in order to determine the optimum strain rate at which the steel behaves superplastically. An INSTRON 1195 model equipment for traction test with a load capacity of 100 kN was used along with an INSTRON 3112 model furnace which allows reaching temperatures as high as 1000°C. The tests were made without a protective atmosphere at speeds between 0.05 and 10 mm/min (strain rates in the range of  $10^{-3} - 10^5 s^{-1}$ ). Before the tests were performed, uniform heating from room to test temperature was made, lasting 1 hour, followed by a 5~10 min of stabilization. Variations of temperature inside the furnace were of maximum  $\pm 10^\circ C$ .

Considering the expression  $\sigma = K \dot{\epsilon}^m$  (where  $K$  is a function of the temperature), the previous deformation the steel may have suffered and the grain size, coefficient  $m$  expresses the sensitivity of the applied tension to strain rate as follows:

$$m = \left( \frac{\log(\sigma_{y_2} / \sigma_{y_1})}{\log(\dot{\epsilon}_{0_2} / \dot{\epsilon}_{0_1})} \right)_{T,d,\epsilon} \quad (1)$$

being  $\sigma_y$  and  $\dot{\epsilon}_0$  the yield stress at 0.2% and the initial strain rate, in tests made at two different strain rates.

Metallographic observations were carried out before and after the high temperature tests were made, analyzing the transverse sections of the samples in an axis parallel to the rolling direction. For most of the samples, normal grinding, polishing and etching with Nital-2 solution procedures were used. A Nikon Epiphot metallographic equipment connected to a Buehler Omnimet image analyzer, which allows the automated counting of features using linear intersection techniques and point counting over a mesh superposed to the microstructure image at 400 and 600x were used in the analysis in order to determine the ASTM grain size and its distribution of either all the grains of the steel or only the ferrite. A sufficient amount of micrographs (a minimum of 5), was used during counting. The metallographic observation was also used to analyze different types of structural damages produced during superplastic deformation of selected samples. A scanning electron microscope (SEM) JEOL JSM-5600 with an electroprobe analyzer OXFORD model 6587 was used to observe characteristics such as decohesions and identify small precipitates.

Figure 1 presents the engineering tensile curves for samples tested at six different temperatures and a crosshead speed of 5 mm/min. As expected, the higher the temperature the lower the maximum stress the sample may withstand, which for 600°C is above 200 MPa and for 900°C is below 80 MPa. It is noteworthy that at 800°C the elongation of the sample is higher than 100%.

In figure 2, as the crosshead speed is 10 times lower than in figure 1, the steel shows lower maximum stresses and for 600, 650 and 750°C, the evidence of more than one necking phenomena results in descending and ascending zones. Again, at 800°C the elongation surpasses 100%.

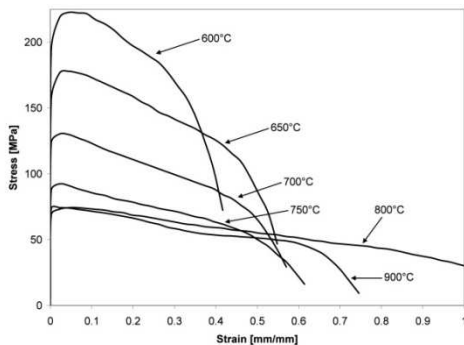


Figure 1: Engineering stress-strain curves at different temperatures and 5 mm/min crosshead speed

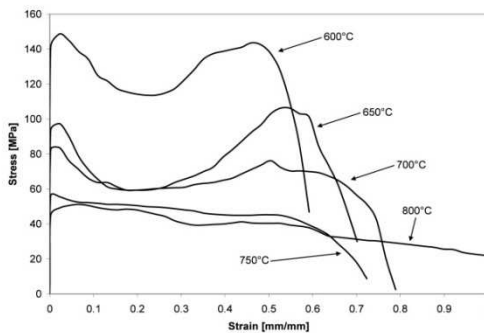


Figure 2: Engineering stress-strain curves at different temperatures and 0.5 mm/min crosshead speed

Considering an even lower crosshead speed (figure 3), the low strain rate promotes at 650 and 700°C the formation of multiple necks shown as ripples in the curves. All these figures indicate that a temperature above 750 and below 850°C results in a smooth deformation and very high elongations of the sample which is an indication of superplasticity.

Once figures 1, 2 and 3 were analyzed and 800°C was determined as a temperature in which the material may present superplastic behavior, tensile tests at different crosshead speeds were made with this temperature value (figure 4). Though some ripples are evident during deformation at 5 mm/min, this phenomenon is increased at 0.5 mm/min. The smooth deformation of the samples is only achieved when the crosshead speed is lowered to 0.2 mm/min. For 0.2 and 0.1 mm/min, the elongation of the samples is close to 200%. Table I presents the results obtained from the tensile tests made at 800°C at different strain rates and different types of tests (tension, superplastic and creep tests).

	L (mm)	V <sub>t</sub> (mm/min)	σ <sub>y</sub> (MPa)	A (%)	ε̇	log(ε̇)	log(σ <sub>y</sub> )
Non	57	5	70.0	109.2	1.46E-03	-2.84	1.845

<b>Superplastic tests</b>	30	0.5	57.3	92.7	2.78E-04	-3.56	1.758
	57	0.5	45.8	111.4	1.46E-04	-3.84	1.660
<b>Superplastic tests</b>	30	0.2	52.8	191.3	1.10E-04	-3.96	1.723
	57	0.2	37.6	>110.0	5.85E-05	-4.23	1.575
	<b>30</b>	<b>0.1</b>	<b>34.4</b>	<b>181.7</b>	<b>5.56E-05</b>	<b>-4.25</b>	<b>1.537</b>
	30	0.05	27.4	137.5	2.78E-05	-4.56	1.438

Table I: Tests made at 800 °C using different strain rates

The microstructural analysis of the steel in its raw state (figure 5), along with the analysis of grain size distribution, shows a 12 ASTM G grain size mean value, which corresponds to approximately 5  $\mu\text{m}$ . This value is small enough for the material to show, under the proper conditions of temperature and strain rate, a superplastic behavior. It is also evident from figure 5 that the hot rolling direction (horizontal axis) produces ferrite and pearlite bands and oriented microstructure.

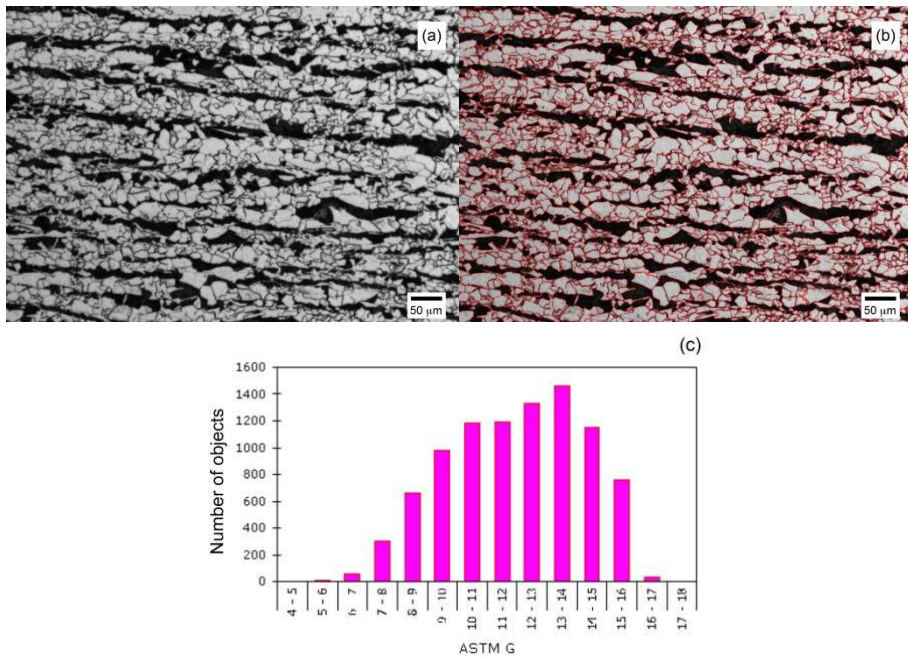


Figure 5: Hot rolled raw state microstructure (a), detected grain pattern (b) and ASTM G grain size distribution histogram (c)

On the other hand, figure 6 presents the same analysis on the hot rolled raw state material, but only measuring the ferrite grains. The mean value of the ferrite grains distribution is closer to 13 ASTM G, which means that the small and soft ferrite grains are responsible for the superplastic behavior.

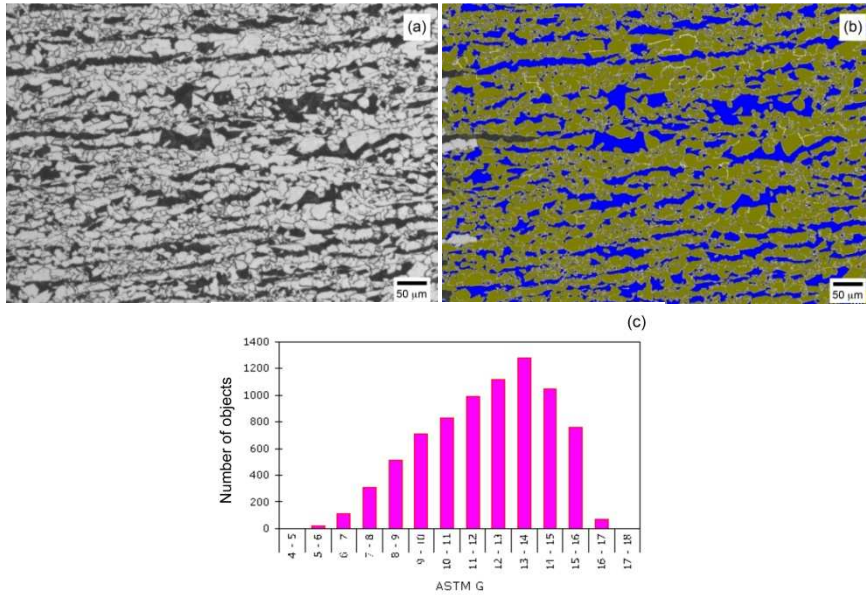


Figure 6: Hot rolled raw state microstructure (a), detected ferrite phase (b) and ASTM G ferrite grain size distribution histogram (c)

Figure 7 shows the microstructure of a sample after being superplastically deformed at 800°C (0.1 mm/min crosshead speed) at a zone 15 mm from the rupture of the specimen. The banded oriented structure has almost disappeared and restored ferrite grains are observed. Also, figure 8, shows characteristics of the structure at the same zone with evidence of decohesion between the ferrite and/or the ferrite-pearlite grains of different types. These are evidence of superplastic mechanisms acting during deformation of the sample [19].

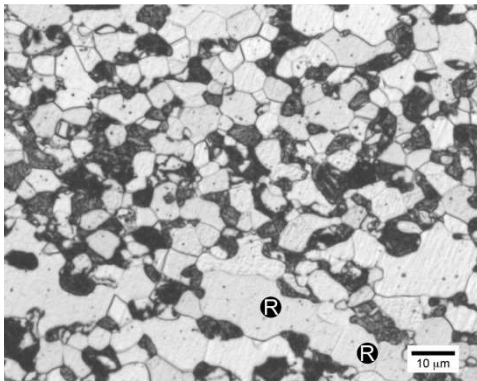


Figure 7: Micrograph of a specimen superplastically deformed at 800°C at a zone close to rupture (15 mm away from it). Restored ferrite (R) is observed.

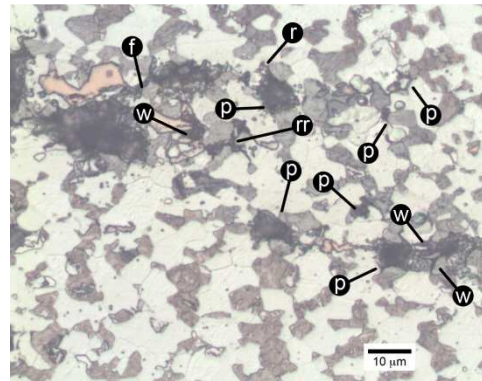


Figure 8: Micrograph of a specimen superplastically deformed at 800°C at a zone close to rupture (15 mm away from it). w-shaped decohesion between ferrite-ferrite-pearlite (w), rr-shaped decohesion between ferrite and pearlite (rr), ferrite-pearlite decohesion (f) and ferrite-ferrite (r) or pearlite-pearlite decohesion (p) are observed.

**3. Discussion.-** The tension testing of the steel at high temperature indicates that both the temperature of the test and the strain rate must be adequate to obtain a superplastic behavior (approximately 200% of elongation). Though the curves shown in figure 1 have the usual shape of a tension test, as strain rate becomes lower (figure 2), uncommon behavior, represented by the formation of more than one neck during plastic deformation, becomes evident. Moreover, it is

clear that at 800°C (figures 1, 2 and 3) the material shows elongations with higher values in comparison to other temperatures.

The microstructure of the steel shown in figure 5 is formed by ferrite and pearlite bands, which are features commonly found in construction steels that were modified by a peritectic reaction and solidification under non-equilibrium conditions. As the partition coefficient for carbon, alloying elements (Mn and Si) and impurities (P, S) in this steel, is lower than one, the microstructure cannot be regenerated during soaking treatment before hot-rolling [20]. Figure 9 shows a comparison between the material in its hot rolled raw state (a) and after tension tested (b). In the initial microstructure both ferrite and pearlite grains are continuous and elongated in the rolling direction, while the ferritic volume fraction is higher than the pearlitic one, which is ~30%. On the other hand, the microstructure of the high temperature tested specimen shows the following:

- crystals of ferrite and pearlite, homogeneously distributed as there is a rearrangement of the initial banded structure,
- grain size remains stable (~13 ASTM).

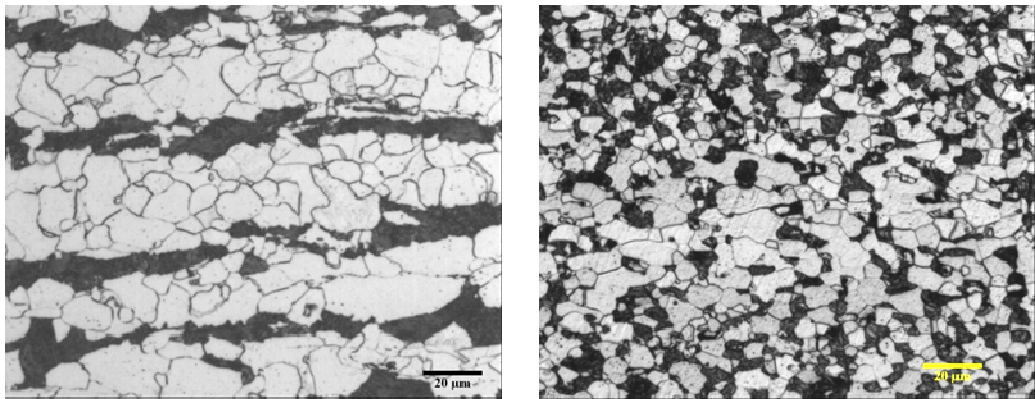


Figure 9: Microstructure of steel in its Hot Rolled Raw State Condition (a) and the steel tested at 800°C and  $5.5 \times 10^{-5} \text{ s}^{-1}$  strain rate (b)

If the superplastic behavior models [21] are used to analyze the relation of stress with strain rate (figure 10), it is evident that:

- A zone II behavior is observed.
- The transition from zone I (creep) to zone II is not evident as tests at lower strain rates should be made in order to observe it.
- At higher strain rates, zone III behavior emerges [6].

The regression lines, also indicated in figure 10a, have slope values of ~0.6 for zone II and ~0.1 for zone III. When the strain rate sensitivity coefficient  $m$  lies between 0.3 and 0.7, superplasticity is achieved, figure 10b.

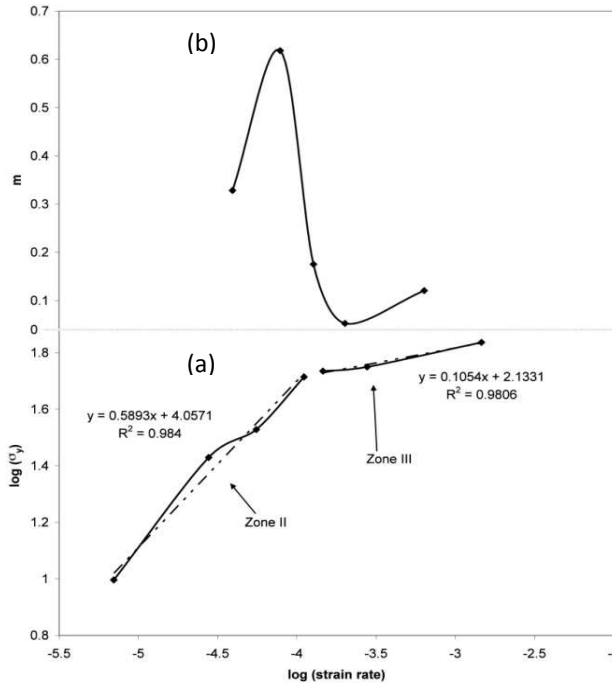


Figure 10: Influence of strain rate on yield stress (a) and superindex  $m$  (b) of equation (1) in superplastic behavior at 800°C.

Ashby and Verrall have proposed the following constitutive equation that relates tension, strain rate, grain size and temperature [6]:

$$\dot{\epsilon} = \frac{98\Omega}{kT d^2} \left[ \sigma - \frac{0.72\Gamma}{d} \right] D_v \left[ 1 + \frac{\pi \delta}{d} \frac{D_B}{D_v} \right] \quad (2)$$

where  $\dot{\epsilon}$  is strain rate,  $\Omega$  atomic volume of ferrite,  $T$  absolute temperature,  $k$  Boltzmann constant,  $\sigma$  applied stress,  $\Gamma$  interfacial  $\alpha/\alpha$  energy,  $d$  grain size,  $D_v$  diffusion coefficient for the ferrite volume,  $\delta$  grain boundary thickness and  $D_B$  diffusion coefficient for the ferrite grain boundary. For ferrite, at 800°C, the values of  $D_v$ ,  $\Omega$ ,  $\Gamma$  and  $\delta$  are approximately  $4 \times 10^{-16} \text{ m}^2/\text{s}$ ,  $12.2 \times 10^{-30} \text{ m}^3$ ,  $0.6 \text{ J/m}^2$  and  $5 \times 10^{-10} \text{ m}$  respectively [22].

An approximate value for the diffusion coefficient (equation (2)) can be calculated through data ( $\sigma, \dot{\epsilon}$ ) of the material deformed in superplastic conditions obtained in tests at 750 and 800°C. An approximation to the previous formula for constant grain size (5µm in this case) is the following:

$$\dot{\epsilon} \propto \sigma^n \exp\left(-\frac{Q}{RT}\right) \quad (3)$$

where  $Q$  is the activation energy for the diffusion,  $R$  is the constant for ideal gasses and  $n$  is a coefficient approximately equal to  $1/m$  [10].

Equation (3) results in:



$$\frac{\dot{\epsilon}_{800}}{\dot{\epsilon}_{750}} = \left( \frac{\sigma_{y800}}{\sigma_{y750}} \right)^n \exp \left[ -\frac{Q}{R} \left( \frac{1}{1073} - \frac{1}{1023} \right) \right] \quad (4)$$

And using the data:  $\dot{\epsilon}_{800} = 5.56 \times 10^{-5} s^{-1}$  and  $\sigma_{y800} = 34.4 MPa$  at  $800^\circ C$  (1073 °K) and  $\dot{\epsilon}_{750} = 2.92 \times 10^{-5} s^{-1}$  and  $\sigma_{y750} = 32.47 MPa$  at  $750^\circ C$  (1023 K) for  $m \approx 0.3$  (superplastic behavior threshold), results in a value of  $Q \approx 97050.024 J/mol$  [22]. Therefore,

$$D \propto 10^{-4} \left( \frac{m^2}{s} \right) \exp \left( -\frac{97050024}{8.314 \cdot 1073} \right) = 1.8851 \times 10^{-9} = 4 \times 10^{-16} \left( 1 + \frac{\pi(5 \times 10^{-10}) D_B}{5 \times 10^{-6} D_V} \right) \quad (5)$$

Where

$$\frac{\pi \delta D_B}{d D_V} \propto \frac{1.8851 \times 10^{-9}}{4 \times 10^{-16}} \frac{\pi(5 \times 10^{-10})}{5 \times 10^{-6}} \propto 1.5 \times 10^3 \text{ (at } 800^\circ C) \quad (6)$$

In other words, the diffusivity in grain boundaries is three orders of magnitude higher than the bulk diffusivity. This calculation confirms that the diffusion through grain boundaries is the one ruling the process of intergranular sliding in superplasticity, which has also been concluded by other authors [23].

Figure 7 presents the microstructure after deformation: there are ferrite grains of a larger size, slightly elongated in the rolling direction, with evidence (subgrains) of having suffered dynamic recovery during deformation. Furthermore, figure 8 shows:

- decohesions shaped as w and r, mainly located in the ferrite/pearlite (previous austenite grains) interphase, which is an unequivocal proof of intergranular sliding during the deformation process.
- small cavities in the  $\alpha$ -pearlite (previous austenite grains) interphase, which shows different deformation capacity for each of these phases.
- null evidence of generalized grain growth during deformation, as grain size is very similar to the original one.
- grain (or grain groups) sliding and rotating, a consequence of superplastic deformation.

During superplastic deformation, the decohesions of the ferrite and pearlite bands occur as a consequence of intergranular sliding of the ferrite within the austenite grains (the two components of the steel at the deformation temperature), as shown in figure 11a by SEM analysis. Superplastic flow stops when the intergranular damage and decohesions between matrix and inclusions take place leading to a ductile fracture (figure 11b).

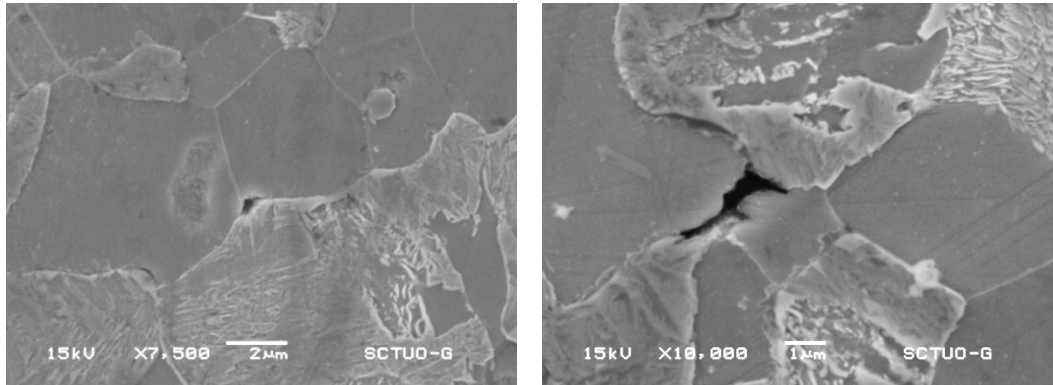


Figure 11: Decoherions or microcavitations between the ferrite and pearlite during superplastic deformation (R-shaped crack) (a) and as a consequence of a conventional high-temperature deformation (decoherions between matrix and hard constituent) (b).

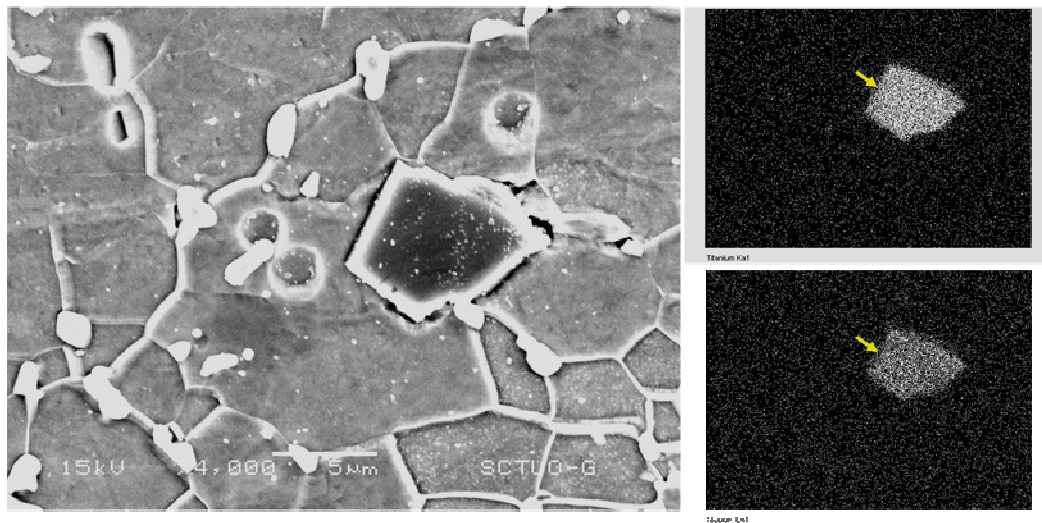


Figure 12: SEM micrograph showing a titanium carbonitride and niobium carbide.

The role of decoherions is evident if the role of Ti and Nb carbides (or carbonitrides) is taken into account as these particles are not dissolved during the 800°C test (figure 12), as these precipitates anchor the grain boundary and prevent the grain growth during rolling, which is accompanied by the formation of  $\gamma$  - pancaked grains and deformation bands. Consequently, a larger number of nucleation sites are made available for the  $\gamma \rightarrow \alpha$  transformation. This allows the formation of an ultrafine microstructure, fulfilling the requirements for both strength and toughness [24,25].

**4. Conclusions.-** Commercial weldable HSLA steels microalloyed with Ti/Nb and obtained by ATMCRP present ultrafine grained microstructures and superplastic behavior (elongations higher than 100%) when deformed in the ferrite-austenite region at temperatures in the range of 750-800°C with strain rates between  $10^{-3}$  and  $10^{-5} \text{ s}^{-1}$ .

The Ashby-Verrall model is suitable to describe the superplastic behavior of the steel. The most important feature of this model is the grain boundary sliding (GBS) and rotation, along with bulk crystal diffusion to maintain the continuity of the steel. The optimum superplastic behavior is found at 800°C with a strain rate of  $10^{-4} \text{ s}^{-1}$ .

The Ashby-Verrall Model is confirmed through the existence of decohesions, as a consequence of massive sliding during deformation, leading to localized necking and failure. Though these steels may show superplastic deformation at high temperature, this deformation does not imply a generalized grain coarsening of the microstructure even when the strain rate is very low ( $10^{-5} \text{ s}^{-1}$ ).

**5. Acknowledgments.-** The authors thank the Department of Metal Sheet and Hot Coil of Mittal Arcelor of Gijón – Avilés (Asturias, Spain) for providing samples for this research. Also to T. Iglesias and B. Mendieta for the preparation of images and figures.

## 6. References

- [1] Backofen, W.A.; Turner, I.R. and Avery, H. *Superplasticity in an Al-Zn Alloy*. Trans ASM, 1964, vol. 57, pp. 980-990.
- [2] Sherby, O.D.; Wadsworth, J. and Oyama, T. *Superplasticity: Prerequisites and Phenomenology*. U.P. Madrid. Madrid : s.n., 1985. E.T.S.I.C.C.P.
- [3] Alden, T.H. *Plastic deformation of materials. Review Topics in Superplasticity*, NY Academic Press, NY, USA, 1975, pp. 225-266.
- [4] González, R., García, J.O., Barbés, M.A., Quintana, M.J., Verdeja, L.F., Verdeja, J.I. *Ultrafine Grained HSLA Steels for Cold Forming*. J Iron Steel Research Int, 2010, vol. 17, num. 10, pp. 50-56.
- [5] Avery, D.H. and Backofen, W.A. Trans ASM, 1965, vol. 58, pp. 551-562.
- [6] Ashby, M.F. and Verrall, R.A. *Diffusion-accomodated flow and superplasticity*, Acta Metall Mater, 1973, vol. 21, p. 149.
- [7] Pero-Sanz, J.A. *Science and Materials Engineering*, CIE–Dossat 2000, Madrid, Spain, 2006, pp.
- [8] Projects: ULSAB, <http://www.ulsab.org/Projects/ULSAB.aspx>, (2012).
- [9] Mukherjee, K.; Hazra, S.S. and Militzer, M. *Grain refinement in dual-phase steels*, Met and Mat Trans A, 2009, vol. 40A, pp. 2145-2159.
- [10] Quintana, M.J., Gonzalez, R.; Verdeja, L.F. and Verdeja, J.I. *Dual-Phase Ultrafine-Grained Steels Produced by Controlled Rolling Processes*, Materials Science and Technology (MS&T) 2011, Ohio, USA, 2011, p. 504
- [11] Howe, A.A. *Ultrafine grained steels: industrial prospects*, Mater Sci Tech Ser, 2000, vol. 16, pp. 1264-1266.
- [12] Gonzalez, R.; Quintana, M.J.; Verdeja, L.F. and Verdeja, J.I. *Ultrafine grained steels and the n coefficient of strain hardening*, Memoria de Trabajos de Difusion Cientifica y Tecnica, 2011, vol. 9, pp. 45-54.
- [13] Backofen, W. A.; Turner I. R. and Avery, H. *Superplasticity in an Al-Zn Alloy*, Trans ASM, 1964, vol. 57, pp. 980-990.
- [14] Backofen, W. A. *Deformation processing*, Met Trans., 1973, vol. 4, pp. 2679–2699.
- [15] Baudalet, B. *La Superplasticite et la mise en Forme des materiaux*, Memoires Scientifiques Revue Metalurgie, 1971, vol. 68, pp. 479-487.
- [16] Morrison, W.B. *Superplasticity of Low-Alloy Steels*, Trans ASM, 61 (1968), 423-434.
- [17] Reed–Hill, R.E. *Creep. Physical Metallurgy Principles*, Cengage Learning, Independence, KY, 2nd ed., 1994, pp. 827–887.
- [18] Vetrano, J.S. *Superplasticity: Mechanisms and applications*, JOM, 2001, vol. 3, p. 22.
- [19] Pero-Sanz, J. A. *Steels: Physical Metallurgy. Selection and Design*, CIE–Dossat 2000, Madrid, Spain, 2004. (in Spanish)

- [20] Furuhashi, T. and Maki, T. *Grain boundary engineering for superplasticity in steels*, J Mater Sci, 2005, vol. 40, pp. 919-926.
- [21] Davies, G.J.; Edington, J.W.; Cutler, C.P. and Padmanabhan, K.A. *Superplasticity: A Review*, J Mater Sci, 1970, vol. 5, pp. 1091-1102.
- [22] Porter, D.A. and Easterling, K.E. *Phase Transformations in Metals and Alloys*, Chapman & Hall, London, UK, 2<sup>nd</sup> ed., 1996.
- [23] Frommeyer, G. and Jiménez, J.A. *Structural Superplasticity at Higher Strain Rates of Hypereutectoid Fe-5.5Al-1Sn-1Cr-1.3C Steel*, Met and Mat Trans A, 2005, vol. 36A, pp. 295-300.
- [24] Vervynckt, S.; Verbeken, K.; López, B. and Jona, J.J. *Modern HSLA steel and role of non – recrystallisation temperature*, International Materials Review, 2012, vol. 57, pp. 187-207.
- [25] Pero-Sanz, J.A.; Sancho, J.P.; Verdeja, J.I. and L.F. Verdeja, *Ferritic grain size: an ignored factor, in fact, in the failure analysis of the sinking of a famous ship*, DYNA, 2012, vol. 174, pp. 156-161.